Journal of Advances in Medicine and Medical Research

33(17): 192-201, 2021; Article no.JAMMR.71616
ISSN: 2456-8899
(Past name: British Journal of Medicine and Medical Research, Past ISSN: 2231-0614, NLM ID: 101570965)

Magnetic Resonance Imaging with Diffusion Tractography in Assessment of Cerebral Lesions Affecting the Optic Radiations

Nayera Mohamed El-Ganainy[1*], Samah Ahmed Radwan[1], Ehab Mohamed El-Gamal[2] and Mohamed Fouad Sherif[1]

[1]Radiodiagnosis Department, Faculty of Medicine, Tanta University, Tanta, Egypt.
[2]Neurosurgery Department, Faculty of Medicine, Tanta University, Tanta, Egypt.

Authors' contributions

This work was carried out in collaboration among all authors. All authors read and approved the final manuscript.

Article Information

DOI: 10.9734/JAMMR/2021/v33i1731044
Editor(s):
(1) Dr. Ashish Anand, GV Montgomery Veteran Affairs Medical Center, University of Mississippi Medical Center, William Carey School of Osteopathic Medicine, USA.
Reviewers:
(1) Nilesh Bhaskarrao Bahadure, Sanjay Ghodawat University, India.
(2) Priscilla Das, SEGi University, Malaysia.
Complete Peer review History: https://www.sdiarticle4.com/review-history/71616

Original Research Article

Received 01 June 2021
Accepted 06 August 2021
Published 07 August 2021

ABSTRACT

Background: The combination of Functional magnetic resonance imaging with Diffusion Tensor Imaging has proven scientific and clinical relevance. By measuring the directed provides complementary information on white matter architecture, i.e., on the course and integrity of functionally important white matter tracts. In the diffusion of protons along myelinated fibers, Diffusion Tensor neuroimaging research is mainly applied to study the human brain's structural connectivity, whereas diffusion tensor tractography is often also employed for clinical applications. Diffusion Tensor Imaging measurements can be obtained together with Functional magnetic resonance imaging in the same scanning session, which gives an even more complete picture of each patient's brain. This study aimed to assess cerebral lesions affecting optic radiations by magnetic resonance imaging with diffusion tensor imaging tractography.
Methods: Our prospective study was conducted on 30 cases ages ranged from 17-83 years, 10 of them were normal and considered as the control group and 20 patients were presented with clinical neurological symptoms and signs associated with visual abnormalities.

**Corresponding author: E-mail: Nayeraelganainy510@gmail.com;*

Results: There is a significant difference between the Fractional anisotropy difference and difference ratio between the two groups with a p-value of 0.016 and 0.017 respectively. There was a strong significant positive correlation between Fractional anisotropy difference ratio (%) and tractography; r = 0.716 (95% confidence interval: 0.470 - 0.858) and p-value <0.001. We correlated the pathological types with different patterns of tractography. optic radiations fiber tracts were displaced in 83.3% of benign tumors and infiltrated in 16.3%. while in malignant tumors optic radiations fiber tracts were displaced in 75%, infiltrated in 12.5%, and disrupted in 25%. There is no "gold standard" for in vivo tractography. Diffusion Tensor Imaging is the only method that permits the calculation and visualization of fiber tracts trajectories in vivo.
Conclusions: Diffusion Tensor Imaging tractography is clinically feasible and provides useful information regarding the site of optic radiations and their affection by different brain lesions also, surgical strategy for lesions located in eloquent visual areas. Also, there was a strong significant positive correlation between Fractional anisotropy difference ratio (%) and tractography distribution. Also, probabilistic multifiber tractography applied to diffusion Magnetic resonance imaging data acquired at 3T may be better as it can cope with crossing and kissing fibers than deterministic models because it allows many more possible local pathway orientations for each Diffusion Tensor Imaging sample point.

Keywords: Magnetic resonance imaging; diffusion tractography; cerebral lesions; optic radiations.

1. INTRODUCTION

The visual pathway consists of a series of cells and synapses that carry visual information from the environment to the brain for processing [1].

The human visual pathway consists of two neuron chains that traverse the brain anteroposterior in an axial plane, Optic nerve fibers project from the retina to the lateral geniculate nucleus (LGN) of the thalamus via the optic chiasm and optic tracts, From the LGN, fibers emerge as the optic radiation (OR) carrying information from the contralateral visual field (geniculocalcarine tract or the geniculostriate pathway) and traverse the retroarticular portion of the internal capsule on their way to their destination in primary visual cortex in the occipital lobe [2].

Optic radiations (ORs) are two eloquent white matter (WM) fiber bundles that carry visual information from the lateral geniculate nuclei (LGNs) to the occipital visual cortex. Each OR maintains a retinotopic organization of visual information from ipsilateral temporal and contralateral nasal retinal visual fields. These bundles, arising from LGN, pass through the temporal lobe and reach the primary and secondary occipital striate cortices (V1 and V2) as well as the extrastriate occipital cortices (V3, V4, and V5). OR fibers are grossly divided into three different bundles posterior, central, and anterior, the latter known also as Meyer's loop [3].

Brain function is indirectly assessed with high spatial resolution via detection of local hemodynamic changes in capillaries and draining veins of the so-called functional areas, e.g., regions of the human brain that govern motor, sensory, language, or memory functions [4].

Diffusion tensor imaging (DTI) is an MR imaging technique that relies on the anisotropic diffusion of water Molecules in and alongside nerve axons, which results in a raw Image of the pathways that represents their anatomy [5].

Application of this technique to the human brain can provide unique in vivo visualization of WM architecture. DTI fiber tractography (DTI-FT) is a mathematical technique to reconstruct WM tract representations in three-dimensional (3D) space based on DTI [6].

DTI methods have been applied to various clinical conditions including ischemic injury of optic pathways, multiple sclerosis and optic neuritis, neuromyelitis optica, diabetes mellitus, glaucoma, amblyopia, blindness, cerebral palsy, and neoplastic involvement of optic pathways [7].

DTI is constantly validated, challenged, and developed in terms of acquisition scheme, image processing, analysis, and interpretation. While DTI offers a powerful tool to study and visualize WM, it suffers from inherent artifacts and limitations [8].

Three-dimensional (3D) tractography of the entire human visual system might be more useful in preoperative and/ or intraoperative neurosurgical planning to preserve structural integrity and avoid visual field defects by

mapping the ORs as well as for quantitative assessment of visual recovery after surgery [9].

The combination of fMRI with DTI has proven scientific and clinical relevance. By measuring the directed provides complementary information on WM architecture, i.e., on the course and integrity of functionally important WM tracts. In the diffusion of protons along myelinated fibers, DTI neuroimaging research, DTI is mainly applied to study the human brain's structural connectivity, whereas diffusion tensor tractography (DTT) is often also employed for clinical applications. DTI measurements can be obtained together with fMRI in the same scanning session, which gives an even more complete picture of each patient's brain [10].

This study aimed to assess cerebral lesions affecting ORs by MRI with diffusion tensor imaging tractography.

2. PATIENTS AND METHODS

Our prospective study was conducted on 30 cases ages ranged from 17-83 years, 10 of them were normal and considered as the control group and 20 patients were presented with neurological and visual signs referred to MR units of the Radiodiagnosis department at Tanta university from the Neurosurgery department at Tanta University Hospital as well as from the outpatient neurosurgery clinics between December 2018 and October 2020.

Inclusion Criteria were patients with clinical neurological symptoms and signs associated with visual abnormalities: headache, vomiting, nystagmus, blurring of vision, diplopia, convulsions.

Exclusion criteria were patients who cannot have an MRI scan including Patients with a cardiac pacemaker, non-compatible MRI aneurysm clips, cochlear implants, non-compatible MRI prosthesis, known to have metallic foreign bodies, and claustrophobic patients.

Each patient included in the study was subjected to Full history taking: name, age, sex, habits, occupation, complaint, present history, history, family history. Clinical examination. MR examination.

2.1 Technique

The technique was performed using a standard 1.5 Tesla unit (GE Signa Explorer). A standard head coil was used. Conventional MR examination with or without Pre & post-contrast including 3D SPGR, T2WI, and FLAIR in axial, sagittal, and coronal planes. The sequences obtained then examination started with no delay time and Diffusion Tensor, which consisted of a single shot, a spin-echo echoplanar sequence in 40 encoding directions, and a diffusion weighting factor of 800s/mm2.

2.2 Other Parameters

T1-weighted image (TR<800, TE<30, flip angle: 90 degrees). T2-weighted image (TR>2000, TE>80, flip angle: 90 degrees). Fluid attenuated inversion recovery (FLAIR) image (TR>3000, TE>80, variable angles). Diffusion-weighted image (DWI): TR 10951, TE 67, matrix 128 x128, FOV 224 X 224 mm, number of excitations 2, slice thickness: 2.0/00 and flip angle 90 (degrees). All the diffusion-weighted images were transferred to the workstation (Advantage workstation 4.7) Images were post-processed using the GE software devised for tractography. The maps obtained were: Color-coded maps, 3D fiber tractography maps, and FA maps.

The direction and anatomy of the tracts were seen in the color-coded map, where a specific color is assigned to tracts running in the three orthogonal planes: Red is for the right to left tracts. Green for anteroposterior tracts. Blue for craniocaudal tracts.

A 3D display of tracts was created. For creating 3D fiber tracts, an ROI (or seed) was drawn (placed) along the course of the tract in the (axial, sagittal, or coronal) color-coded map in single or consecutive sections. The software then automatically traces the assigned tract and presented it in a 3D manner.

Regions of interest (ROIs) were drawn within identifiable WM tracts affected by the tumor, avoiding grossly cystic and necrotic regions, known fiber crossings, and gray matter.

Color-coded DTI maps were analyzed, both subjectively by visual comparison with the contralateral side and quantitatively by comparing the FA values of certain well-known anatomical regions followed by tractography of individual tracts. In most patients the tumor was isolated to one hemisphere, the location of each

tract and its hue on directional color maps were classified as normal or abnormal, based on comparison to the homologous tracts in the contralateral hemisphere which were unaffected by the tumor.

2.3 Method of Tracking of Optic Radiation

A deterministic method of fiber tracking for quick tractography based on ROIs placed in the DTI scan. To track the course of the OR, spherical regions of interest (ROI) were used. The ROIs were placed on known anatomical key structures of the OR which were identified on the T2 weighted image. These structures were: the Lateral geniculate body, the lateral wall of the temporal horn, trigonum, and occipital horn of the ventricle system and the visual cortex. These ROIs were defined for both hemispheres, the ROIs were manually placed in the axial slice of color-coded DTI map on the earlier mentioned anatomical key structures to track the OR from the LGB to the visual cortex.

We adopted the criteria developed by Cruz et al in 2007 to classify fiber tract involvement into 4 categories: Deviated (Displaced), Edematous, Infiltrated, and Destructed (Disrupted).

2.3.1 Displacement

Maintained normal anisotropy relative to the contra-lateral tract. Situated in an abnormal location or presented by abnormal orientation. Directional changes are reflected by abnormal hues on directional maps. Identifiable intact fiber tracts.

2.3.2 Invasion

Reduced anisotropy is relative to the contra-lateral tract. Still identifiable fiber tract. Normal orientation on directional color maps.

2.3.3 Disruption

Markedly reduced anisotropy relative to the contra-lateral tract. The fiber tract is unidentifiable on directional color maps.

2.4 Statistical Analysis

Statistical presentation and analysis of the present study were conducted, using the mean, standard deviation, Paired t-test, Chi-square, Linear Correlation Coefficient, and Analysis of variance [ANOVA] tests by SPSS V17. The linear Correlation coefficient was used for the detection of correlation between two quantitative variables in one group. ANOVA test was used for comparison among different times in the same group in quantitative data. The level of significance was adopted at $p \leq 0.05$.

3. RESULTS

The age of patients in the study ranged from 17 to 83 years, mean age was 44.57 ± 13.33, 12 patients (40% of cases) were males and 18 patients (60% of cases) were females Table 1.

Table 1. Patients' characteristics of all studied patients

		Patients (n = 30)
Age (years)	**Mean ± SD**	44.57 ± 13.33
Sex	**Male**	12 (40%)
	Female	18 (60%)

We had 30 cases, 21 of them presented mainly with headache,17 cases with the blurring of vision 8 cases with disturbed conscious level, 1 case with hemiparesis and 4 cases with convulsions,1 case with vomiting, 1 case with behavioral changes, 2 known cases of MS for follow up Table 2.

Table 2. Clinical data of both groups

	Group 1 (n = 20)	Group 2 (n = 10)	P value
Headache	13 (65%)	8 (80%)	0.118
Convulsions	3 (15%)	1 (10%)	
Blurring of vision	17 (85%)	0 (0.0%)	
Disturbed conscious level	8 (40%)	0 (0.0%)	
Behavior changes	1 (5%)	0 (0.0%)	
Vomiting	1 (5%)	0 (0.0%)	
Loss of memory	1 (5%)	0 (0.0%)	
Follow up	2 (10%)	0 (0.0%)	
Hemiparesis	1 (5%)	0 (0.0%)	

Table 3. Fractional anisotropy (FA) of both groups

		Group 1 (n = 20)	Group 2 (n = 10)	P value
FA Difference	Mean ± SD	0.12 ± 0.11	0.03 ± 0.02	**0.016***
FA Difference ratio (%)	Mean ± SD	22.68 ± 18.60	7.41 ± 4.84	**0.017***

Table 4. Relationship between FA difference ratio (%) of affected and contralateral optic radiations

		Patients (n = 20)	P value
Affected optic radiation	Mean ± SD	0.38 ± 0.11	<0.001*
Contralateral optic radiation	Mean ± SD	0.50 ± 0.10	

Table 5. Relationship between tractography distribution and FA difference ratio (%) of both groups

	Normal (n = 11)	Displaced (n = 13)	Infiltrated (n = 2)	Disrupted (n = 4)	P value
Mean (%)	7.24	14.73	30.68	48.82	**<0.001***
SD	4.63	9.00	14.82	21.65	

Table 6. Relationship between pathology and tractography

	Normal	Displaced	Edematous	Infiltrated	Disrupted	p-value
Benign tumor	0	5	0	1	0	0.127
Malignant tumor	0	6	0	1	2	
Neuro demyelinating disorder	1	1	0	0	0	
Neurovascular	0	2	0	0	0	
Neurodegenerative	0	0	0	0	1	

There was a significant difference between FA difference and FA difference ratio between the two groups with a p-value of 0.016 and 0.017 respectively Table 3.

There was a significant difference between FA of the affected side and FA of the contralateral side in the lesion group. Table 4.

There was a strong significant positive correlation between FA difference ratio (%) and tractography; r = 0.716 (95% confidence interval: 0.470 - 0.858) and P value <0.001. Table 5.

OR fiber tracts were displaced in 83.3% of benign tumors and infiltrated in 16.3%. while in malignant tumors OR fiber tracts were displaced in 75%, infiltrated in 12.5%, and disrupted in 25%. Table 6.

4. CASE PRESENTATION

Case No. (1): Meningioma; A 40 years-old female patient presented with a blurring of vision and behavioral changes. (Fig. 1).

Case No. (2): Encephalomalacia; An 83 years-old male patient known presented with disturbed consciousness, blurring of vision, and memory loss. (Fig. 2).

5. DISCUSSION

Age distribution in our study coincides with Coenen et al., 2005 [11] showed that patients with symptomatic lesions from diagnostic imaging that were suspected to affect the OR were included in this study. Their age range was 17–66 years (mean 42.5±21.2) years.

Faust and Vajkoczy, 2016 [12] showed mean patient age in years 54 ± 16 that partially agreed with our study. Takemura et al., 2017 [13] who performed MRI tractography of ORs in patients with MS showed age (mean ± SD year) 47.4 ± 13 in bilateral cases and 39.4 ± 11.5 in unilateral cases that agreed with our study.

Lv, et al. [14] performed MRI tractography in 18 patients with meningioma aged 46 to 65 years

with a mean of 54.5 ± 6.12 years that differed from our study.

As regards sex distribution our study partially agreed with Takemura et al. [13] who reported that sex distribution in their study was male: female 1: 6 in bilateral cases and 2: 5 in unilateral cases. But differed from Coenen et al. [11] that showed four female patients with symptomatic lesions from diagnostic imaging, these were suspected to affect the OR were included in this study and also differed from the study made by Faust and Vajkoczy [12] noted that male/female ratio was 70:43 and differed from Lv et al. [14] who mentioned that the patients were 10 males and 8 females.

The clinical presentations of the patients classified into headache 21 (70.0%), convulsions 4 (13.3%), blurring of vision 17(56.7%), disturbed conscious level 8 (26.7%) behavior changes 1(3.3%), vomiting 1 (3.3%) loss of memory 1 (3.3%), follow up 2 (6.7%), hemiparesis 1 (3.3%).

Yu et al. [15] who studied DTI fiber tracking of lesions adjacent to corticospinal tract mentioned that the clinical presentations of 17 cases are classified into 10 cases headache, 7 cases of motor impairment, numbness, 2 cases seizures, 2 cases of language deficit, 1 case cognitive changes,1case memory loss that agreed with our study.

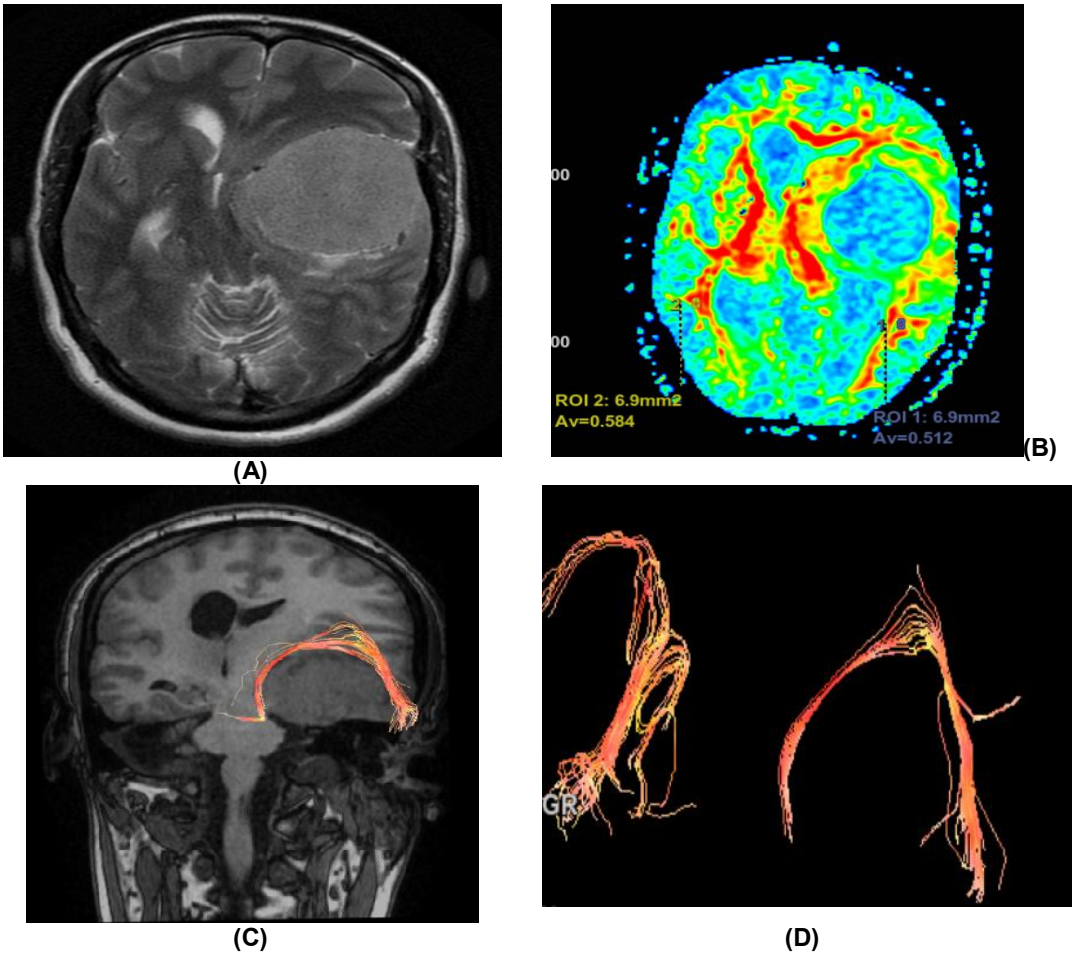

Fig. 1. (A) Axial T2WI image showed left parietal extra-axial space-occupying lesion showed high signal in T2. The lesion effaced the underlying cortical sulci, compressed the left lateral ventricle with secondary subfalcine herniation. (B) Axial FA map showed the affected fibers (left optic radiation) with its FA 0.512 compared to the contralateral intact fibers measured 0.584. 3D fiber tractography image in coronal view (C) & OR view (D) showed displacement and attenuation of the fibers of the left optic radiation and normal fibers of the right optic radiation

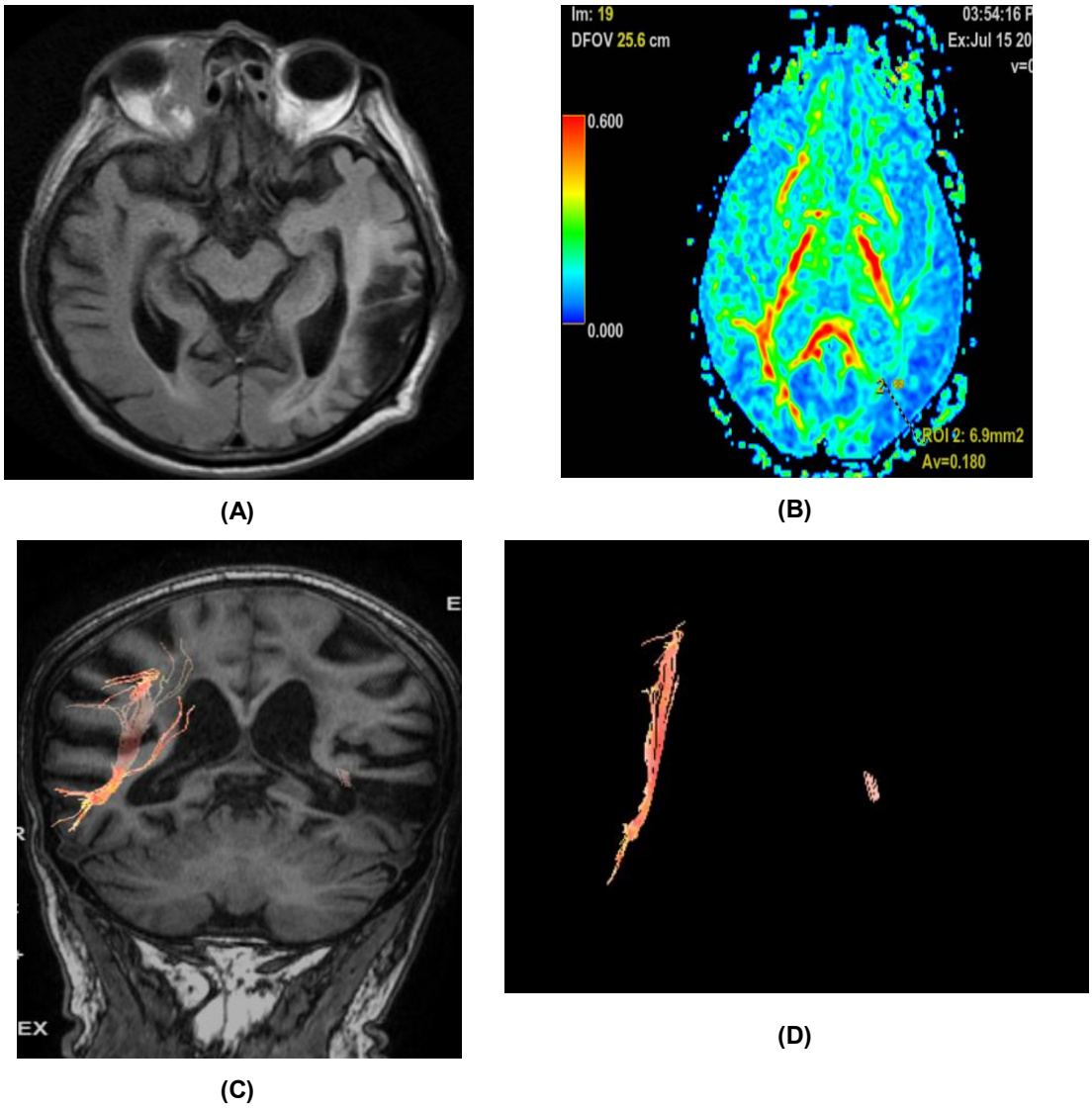

Fig. 2. (A) Axial FLAIR showed left tempro-occipital lesion gliosis with mild exvaca dilatation of occipital horn of lateral ventricle. (B) Axial colored FA map showed that FA of affected fibers (left optic radiation) decreased to 0.180 compared to the contralateral intact fibers measured 0.489. 3D fiber tractography images in coronal view (C) and OR view (D) showed destruction of the left optic radiation fibers to normal right optic radiation fibers

Our study agreed with Tatsuzawa et al. [16] who studied brain tumors adjacent to the OR using diffusion tensor imaging-based tractography classified them into 7 cases Occipital lobe, 5 cases temporal lobe, 2 cases parietal lobe. Also, agreed with Coenen et al. [11] who classified them into1 right temporal, 1 left temporo-occipital,1 left occipital, 1 right occipital, calcarine fissure, but disagreed with Field, A. S et al. [17] who noted that all tumors were limited to one cerebral hemisphere.

Our study agreed with Faust and Vajkoczy, [12] who had 65 cases of glioblastoma multiforme, 16 cases of astrocytoma GIII, 10 cases of astrocytoma GII, 3 cases oligodendroglioma GII, 17 cases with metastasis, and partially agreed with Coenen et al. [11] who had 1 case glioblastoma WHO grade IV, 1 case oligoastrocytoma WHO grade III, 1 case cavernoma and 1 case metastasis.

Pathologic diagnosis reported by Field et al. [17] included four oligodendrogliomas (WHO

classification grade II), three solitary metastases (one each of melanoma, adenocarcinoma, and squamous cell carcinoma), two anaplastic astrocytomas, and one each of the following: glioblastoma multiforme, malignant oligoastrocytoma, pilocytic astrocytoma, and ganglioglioma that disagreed with our study.

We agreed with Meyer et al. [18] who mentioned that Diffusion-weighted MR imaging is highly sensitive for the diagnosis of cerebral infarction. Areas of cerebral infarction have decreased apparent diffusion, which resulted in increased signal intensity on diffusion-weighted MR scans. 12 cases with acute infarction showed hyperintense lesions on diffusion-weighted images. Four cases of chronic infarction one of them was encephalomalacia and reactive gliosis associated with the two chronic strokes seen as low-signal lesions on a diffusion-weighted image.

We disagreed with Kono et al. [19] who reported in this study that signal intensities on DWIs in the solid portion with the hyper intensity seen in 5 cases GBMs, 5 cases astrocytoma, 11 cases of meningioma, iso-intensity seen in 4 cases GBMs, 3 cases astrocytoma, 9 cases meningioma, and low intensity is seen in 2 cases of GBMs and 3 cases meningioma.

Color-coded DTI maps were analyzed followed by fiber tractography of individual tracts. In almost of patients, the lesion was isolated in only one hemisphere, data was obtained by comparing the FA of the affected tract by the lesion and the contralateral tract.

Cruz and Kimura et al. [20] updated the classification into five patterns, classified patterns of WM tract involvement into:

In the same way, our study agreed with Jellison et al. [21] who classified the WM tracts affection into four patterns. Pattern 1: consists of normal or only slightly decreased FA with abnormal location and/or direction resulting from bulk mass displacement. This is the most clinically useful pattern in preoperative planning because it confirms the presence of an intact peritumoral tract that can potentially be preserved during resection. Pattern 2: is substantially decreased FA with normal location and direction (i.e. normal hues on directional color maps). We frequently observe this pattern in regions of vasogenic edema, although the specificity of this pattern is not yet known; further study is needed to determine the clinical utility of this observation. Pattern 3 is substantially decreased FA with abnormal hues on directional color maps. We have identified this pattern in a small number of infiltrating gliomas in which the bulk mass effect appeared to be insufficient to account for the abnormal hues on directional maps. We speculate that infiltrating tumors disrupt the directional organization of fiber tracts to cause altered color patterns on directional maps, but this phenomenon requires further study. Pattern 4 consists of isotropic (or near isotropic) diffusion such that the tract cannot be identified on directional color maps. This pattern is observed when some portion of a tract was completely disrupted by a tumor. This pattern can be useful in preoperative planning in the sense that no special care needs to be taken during resection to preserve a tract that is shown by DTI to be destroyed. It should be noted that combinations of the above patterns may occur; for example, a combination of patterns 1 and 2 may be observed in a tract that is both displaced and edematous.

Our study agreed with Lv et al. [14] who reported that patients were classified into four intervals of the ratio of the FA value for the affected side to that for the healthy side. Patients in the first interval, having a ratio less than 25%, had destruction of the OR; 25-patients in the second interval, having a ratio of 50%, had moderate damage; patients in the third interval, 50 having a ratio of 75%, had a shifted OR; and patients in the fourth interval, having a ratio greater than 75%, had a normal or nearly normal OR. The results of conventional MRI, FA, color-coded tensor maps, and three-dimensional white-matter tracing were compared. The FA value ratio for malignant meningioma patients was 10.5%, corresponding to the first interval, and FA images failed to show the optic-radiation beam, suggesting that WM had been destroyed. The FA value in case 1 was 37.4%, corresponding to the second interval, and the color-coded tensor map and optic radiotracer showed an optic-radiation shift and partial defect. Cases corresponding to the third and fourth intervals only developed an optic-radiation shift or symmetry of the radiation shape, size, position, and color.

Also agreed with Field et al. [17] who stated that four basic patterns of WM alteration: 1) normal or nearly normal FA, with abnormal tract location or tensor directions attributable to bulk mass displacement, 2) moderately decreased FA and with normal tract locations and tensor directions, 3) moderately decreased FA and with abnormal

tensor directions, and 4) near isotropy. FA was inversely correlated for Patterns 1–3 but did not discriminate edema from infiltrating tumors. However, in the absence of mass displacement, the infiltrating tumor was found to produce tensor directional changes that were not observed with vasogenic edema, suggesting the possibility of discrimination based on directional statistics.

But our study disagreed with Yu et al. [15] who announced that disruptive changes were classified according to the integrity of delineated CST in the lesioned hemisphere: complete interruption (CST was not displayed), partial interruption (partial bundle of CST was displayed), or simple displacement (partial bundle of CST was displayed). The partial interruption was evident in seven patients (41.2%) whose lesions were close to the cortex. In the other 10 patients (58.8%), delineated CSTs were intact but distorted. The lesions in these patients were situated near the cerebral peduncle. No complete CST interruption was identified.

In our study, we correlated the pathological types with different patterns of tractography. OR fiber tracts were displaced in 83.3% of benign tumors and infiltrated in 16.3%. while in malignant tumors OR fiber tracts were displaced in 75%, infiltrated in 12.5%, and disrupted in 25%.

This partially agreed with a study done by Ibrahim et al. [22] where there was a statistical difference between these groups, with the prevalence of displacement among the benign group and the disruption among the malignant group; where displacement pattern was seen within (90.9%) of the benign group and within (57.1%) the malignant group. The disruption pattern was seen within (57.1%) of the malignant group and (9.1%) of the benign group.

6. CONCLUSION

DTI tractography is clinically feasible and provides useful information regarding the site of OR and their affection by different brain lesions also, surgical strategy for lesions located in eloquent visual areas. Also, there was a strong significant positive correlation between FA difference ratio (%) and tractography distribution. Also, probabilistic multifiber tractography applied to diffusion MR imaging data acquired at 3T may be better as it can cope with crossing and kissing fibers than deterministic models because it allows many more possible local pathway orientations for each DTI sample point.

ETHIOCAL APPROVAL & CONSENT

The study was approved from Ethical Committee and obtaining informed written consent from patient's.

DISCLAIMER

The products used for this research are commonly and predominantly use products in our area of research and country. There is no conflict of interest between the authors and producers of the products because we do not intend to use these products as an avenue for any litigation but the advancement of knowledge. Also, the research was not funded by the producing company rather it was funded by the personal efforts of the authors.

COMPETING INTERESTS

Authors have declared that no competing interests exist.

REFERENCES

1. Remington L, Goodwin D. Visual Pathway.Clinical anatomy of the visual system. Third Edition ed. 2012;233-52.
2. Joukal M. Anatomy of the human visual pathway. Homonymous visual field defects. Springer. 2017;1-16.
3. Mormina E, Arrigo A, Calamuneri A, Alafaci C, Tomasello F, Morabito R, et al. Optic radiations evaluation in patients affected by high-grade gliomas: a side-by-side constrained spherical deconvolution and diffusion tensor imaging study. Neuroradiology. 2016;58:1067-75.
4. Stippich C. Clinical functional MRI: presurgical functional neuroimaging: Springer; 2015.
5. Wu W, Rigolo L, O'Donnell LJ, Norton I, Shriver S, Golby AJ. Visual pathway study using in vivo diffusion tensor imaging tractography to complement classic anatomy. Neurosurgery. 2012;70:145-56; discussion 56.
6. Nooij RP, Hoving EW, van Hulzen AL, Cornelissen FW, Renken RJ. Preservation of the optic radiations based on comparative analysis of diffusion tensor

imaging tractography and anatomical dissection. Front Neuroanat. 2015;9:96.
7. Kamali A, Hasan KM, Adapa P, Razmandi A, Keser Z, Lincoln J, et al. Distinguishing and quantification of the human visual pathways using high-spatial resolution diffusion tensor tractography. Magn Reson Imaging. 2014;32:796-803.
8. Assaf Y, Pasternak O. Diffusion tensor imaging (DTI)-based white matter mapping in brain research: a review. J Mol Neurosci. 2008;34:51-61.
9. Chen X, Weigel D, Ganslandt O, Buchfelder M, Nimsky C. Prediction of visual field deficits by diffusion tensor imaging in temporal lobe epilepsy surgery. Neuroimage. 2009;45:286-97.
10. Leclercq D, Delmaire C, de Champfleur NM, Chiras J, Lehéricy S. Diffusion tractography: methods, validation and applications in patients with neurosurgical lesions. Neurosurg Clin N Am. 2011;22:253-68, ix.
11. Coenen V, Huber K, Krings T, Weidemann J, Gilsbach J, Rohde V. Diffusion-weighted imaging-guided resection of intracerebral lesions involving the optic radiation. Neurosurgical Review. 2005;28:188-95.
12. Faust K, Vajkoczy P. Distinct displacements of the optic radiation based on tumor location revealed using preoperative diffusion tensor imaging. J Neurosurg. 2016;124:1343-52.
13. Takemura MY, Hori M, Yokoyama K, Hamasaki N, Suzuki M, Kamagata K, et al. Alterations of the optic pathway between unilateral and bilateral optic nerve damage in multiple sclerosis as revealed by the combined use of advanced diffusion kurtosis imaging and visual evoked potentials. Magn Reson Imaging. 2017;39:24-30.
14. Lv X, Chen X, Xu B, Zhang J, Zheng G, Li J, et al. Magnetic resonance diffusion tensor imaging-based evaluation of optic-radiation shape and position in meningioma. Neural Regen Res. 2012;7:686-91.
15. Yu Q, Lin K, Liu Y, Li X. Clinical Uses of Diffusion Tensor Imaging Fiber Tracking Merged Neuronavigation with Lesions Adjacent to Corticospinal Tract: A Retrospective Cohort Study. J Korean Neurosurg Soc. 2020;63:248-60.
16. Tatsuzawa K, Owada K, Sasajima H, Yamada K, Mineura K. Surgical strategy of brain tumors adjacent to the optic radiation using diffusion tensor imaging-based tractography. Oncol Lett. 2010;1:1005-9.
17. Field AS, Alexander AL, Wu YC, Hasan KM, Witwer B, Badie B. Diffusion tensor eigenvector directional color imaging patterns in the evaluation of cerebral white matter tracts altered by tumor. Journal of Magnetic Resonance Imaging: An Official Journal of the International Society for Magnetic Resonance in Medicine. 2004;20:555-62.
18. Meyer JR, Gutierrez A, Mock B, Hebron D, Prager JM, Gorey MT, et al. High-b-value diffusion-weighted MR imaging of suspected brain infarction. AJNR Am J Neuroradiol. 2000;21:1821-9.
19. Kono K, Inoue Y, Nakayama K, Shakudo M, Morino M, Ohata K, et al. The role of diffusion-weighted imaging in patients with brain tumors. AJNR Am J Neuroradiol. 2001;22:1081-8.
20. da Cruz Jr LCH, Kimura M. Diffusion magnetic resonance imaging in brain tumors. Handbook of neuro-oncology neuroimaging: Elsevier. 2016; 273-300.
21. Jellison BJ, Field AS, Medow J, Lazar M, Salamat MS, Alexander AL. Diffusion tensor imaging of cerebral white matter: a pictorial review of physics, fiber tract anatomy, and tumor imaging patterns. AJNR Am J Neuroradiol. 2004;25:356-69.
22. Ibrahim AS, Gomaa M, Sakr H, Abd Elzaher Y. Role of diffusion tensor imaging in characterization and preoperative planning of brain neoplasms. The Egyptian Journal of Radiology and Nuclear Medicine. 2013;44:297-307.

Peer-review history:
The peer review history for this paper can be accessed here:
https://www.sdiarticle4.com/review-history/71616